

# Effects Of Electrode Melting Rate On Safe Welding Fumes In Gas Tungsten ARC Welding

Ibraheem A.P

Achebo .J.I

Ozigagun A

Department of Production Engineering, Faculty of Engineering, University of Benin,  
Benin City, Edo State

*Abstract: The TIG welding processes are accompanied by some of toxic aero-disperse particles which can affect the lungs and respiratory system of welders. This paper has examined Various process parameters affecting electrode melting rate and safe welding fumes in TIG welding. The response surface methodology has been applied to model, examine and explain the influence of current, voltage and gas flow rate on electrode melting rate and fume concentration. Several statistical tools such as box cox plot, cooks distance and surface plots were employed to check for significance, compatibility and strength of the model. The model developed possessed a very high goodness of fit of about 95% determination strength explaining that critical control of gas flow rate is of great importance to reduce the electrode melting rate as well as the fume concentration in TIG welding.*

*Keywords: Fumes, electrode, melting rate, Response Surface Methodology, Tungsten Inert Gas, Welding, Mutation*

## I. INTRODUCTION

Welding is the traditional method of joining metal parts permanently through the application of heat and pressures. There are different types of welding processes such as shielded metal arc welding (SMAW), gas metal arc welding (GMAW) and gas tungsten arc welding (GTAW) or tungsten inert gas (TIG) welding[1].GTAW produces a lesser fumes concentration when compared to GMAW because of its spray transfer mode. Shield gases include argon, helium, or a mixture of active gases including carbon dioxide[2]. The flux cored arc welding (FCAW) process have similar properties like the GMAW. Plasma arc welding (PAW) and FCAW exhibits the highest welding fumes exposure [3]. According to the U.S. EPA, SMAW accounts for 45% of the total welding performed in the U.S., 34% can be accounted to GMAW, and 17% accounts for FCAW welding. Metals commonly found in welding fumes include aluminum, barium, beryllium, hexavalent chromium, chromium oxides, chromium, copper, iron oxide, lead, manganese, magnesium, molybdenum,

nickel, and zinc oxides. Fumes contain silicates and fluorides generated from the electrode-coating emissions. Gases generated by welding include carbon monoxide, nitrogen oxide, and ozone[4]. lower welding fumes concentration are observed in TIG welding ranging between 45 and 77  $\mu\text{g}/\text{m}^3$ .Fumes are solid particles formed by condensation from the gas state. These particles react with air when they are vaporized [2]. Welding fumes particle are, categorized into the ultrafine and fine particle ranges [5]. The particles in this size range are of the respirable fraction. These particle sizes especially affect the lower respiratory tract including the bronchioles and alveoli [6].There is three modes of particle size distribution for aerosols produced while welding. The first captures Fumes less than 1 micrometer made up of oxidized metal vapors are the smallest. These particles are transported in the atmosphere by diffusion and other processes. The next mode includes spherical particles usually between 6 to 13 micrometers that have been solidified from the hot metal that is not oxidized [7]. Reduction of welding fumes can be achieved by use of ventilator, fume hood, exhausts, and use of

personal protective equipment [8]. The shape and size of welding fumes determines the biological activity of the welding fume. Therefore, investigating and understanding the relationship between the welding fume Particle size distribution (PSD) and the arc welding parameters becomes inevitable [9]. Based on numerical methods, research has been done for prediction of particle concentration using Computational Fluid Dynamics (CFD) but the simulated results frequently have some divergence from the experimental results [10]. Fume generated by the shielded metal arc welding (SMAW) process may be a cause for concern due to possible health problems experienced by individuals in the welding industry after long-term exposure. Welding fume particles may cause metal fume fever, and perhaps more importantly, manganese- or chromium related poisoning after inhalation and ingestion into the human body. For example, it has been proposed that long term, low concentration doses of Mn are linked to nervous system disorders[11]. Studies have also shown that welders working with stainless steels who have had cases of lung cancer may be due to possible hexavalent chromium exposure, although there has been no direct evidence linking the cancer to welding fume exposure[12]. Occupational exposure limits (OEL), which are revised quite regularly, determine the amount of these compounds and elements that may be ingested without becoming harmful to human tissues. Though epidemiological reactions to the different compounds present in welding fume are important, they are beyond the scope of this study, which was designed to characterize the fume particles produced by metal joining processes [13].

## II. RESEARCH METHODOLOGY

### A. DESIGN OF EXPERIMENT

To develop optimal solutions an accurate experimental design is very necessary for data collection. Design of experiment is an expert method of combining process parameters optimally using scientific methods, this is determined by the number of input parameters considered. The experimental design considers the following factors such as welding current, gas flow rate, and voltage as input. In this study the experimental matrix was developed using the design expert software, the central composite design was the most suitable for this experiment. The input factors considered and their levels is shown in the table below

Parameters	Unit	Symbol	Coded value	Coded value
			Low (-1)	High(+1)
Current	Amp	A	180	220
Gas flow rate	Lit/min	F	36	42
Voltage	Volt	V	18	24

Table 2.1: Range of input process parameters

Current	Voltage	Gas flow	Fume conc	Electrode melting rate
165.00	17.50	11.50	5	8
165.00	17.50	14.02	29	25
150.00	19.00	13.00	20	13
165.00	17.50	11.50	3.5	6

165.00	17.50	11.50	2	4
165.00	20.02	11.50	1.6	2
180.00	16.00	10.00	1.08	7
139.77	17.50	11.50	11	24
165.00	17.50	11.50	2	5
165.00	14.98	11.50	1.2	0.8
190.23	17.50	11.50	1.1	19
150.00	19.00	10.00	4	3
150.00	16.00	10.00	6	7
180.00	19.00	10.00	4	4
165.00	17.50	11.50	1.8	4.7
165.00	17.50	11.50	1.5	4.25
165.00	17.50	8.98	10	4
150.00	16.00	13.00	11	14
180.00	19.00	13.00	15	22
180.00	16.00	13.00	2	9

Table 2.2: Experimental data

### B. EXPERIMENTAL PROCEDURE

Mild steel plate was used as the base material for the single-pass surface welding with a direct current of reverse polarity. The samples were grinded, sand cleaned and etched to get a fine edge because sample has to be free from grease and dirt. The base metal is welded using the gas tungsten arc welding process with continuous generation of fumes, and all the measurements are done 10 min after the commencement. 100 pieces of mild steel coupons was produced for this experiment using 100% argon gas as the shielding gas. In this process the tungsten non consumable electrode having diameter 3 mm was used alongside a 2 mm diameter filler metal ER309L. The welding fume plume was localized by extracting air at a distance of 40 cm from the welding arc and redirected into the vertical pipe The welding fume dispersion was measured using the laser aerosol spectrometer LAS-P (LAS-P, 2010). The welding fumes are collected using a fume box and also measured the electrode melting rate respectively.

### C. MATERIALS USED FOR THE EXPERIMENT

Low carbon steel popularly known as Mild Steel is one of the most common of all metals used in the fabrication projects.

The choice of mild steel was made because of its affordability, availability, durability, having less than 2 % carbon, gives it a high magnetic quality which supports the weldability of mild steel.



Figure 2.1: welded torch



Figure 2.2: welding fume collection chamber



Figure 2.3: welded samples

### III. RESULTS AND DISCUSSION

In this study, an attempt is made to develop a second order mathematical model to explain the relationship between; current (I), voltage (V) and gas flow rate to reduce fume concentration and electrode melting rate, using response surface methodology (RSM). The first step taken in modeling of an RSM model is to validate the suitability of the quadratic model in analyzing the experimental data, and the the sequential model sum of squares was calculated to check for the best model, electrode melting ratel sum of squares is in table 3.1.

Source	Sum of Squares	df	Mean Square	F Value	p-value	
Mean vs Total	158.89	1	158.89			
Linear vs Mean	9.02	3	3.01	2.69	0.0808	
2FI vs Linear	1.76	3	0.59	0.47	0.7054	
Quadratic vs 2FI	14.92	3	4.97	42.78	< 0.0001	Suggested
Cubic vs Quadratic	0.63	4	0.16	1.80	0.2471	Aliased
Residual	0.53	6	0.088			
Total	185.75	20	9.29			

Table 3.1: Sequential model sum of square for electrode melting rate

In table 3.1 the quadratic model was selected as the most suitable as having the lowest p-value < 0.0001. In assessing the strength of the quadratic model towards minimizing the

electrode melting rate one way analysis of variance (ANOVA) table was generated which is presented in table 3.2.

Source	Sum of Squares	Df	Mean Square	F Value	p-value	Prob > F	
Model	25.70	9	2.86	24.56	< 0.0001		significant
A-current	6.465E-003	1	6.465E-003	0.056	0.8183		
B-voltage	0.055	1	0.055	0.48	0.5061		
C-gas flow rate	8.96	1	8.96	77.03	< 0.0001		
AB	0.55	1	0.55	4.72	0.0550		
AC	7.080E-004	1	7.080E-004	6.089E-003	0.9393		
BC	1.21	1	1.21	10.42	0.0090		
A^2	9.18	1	9.18	78.96	< 0.0001		
B^2	2.67	1	2.67	22.95	0.0007		
C^2	2.29	1	2.29	19.73	0.0013		
Residual	1.16	10	0.12				
Lack of Fit	0.69	5	0.14	1.48	0.3396		not significant
Pure Error	0.47	5	0.094				
Cor Total	26.86	19					

Table 3.2: ANOVA table for electrode melting rate

The anova table shows us the process parameters having the most significant influence on the minimization of the electrode melting rate and the gas flow rate is observed to have a very significant effect on the response with a p-value of < 0.0001. To validate the adequacy of the quadratic model based on its ability to reduce the electrode melting rate the goodness of fit statistics presented in table3.3

Std. Dev.	0.34	R-Squared	0.9567
Mean	2.82	Adj R-Squared	0.9178
C.V. %	12.10	Pred R-Squared	0.7611
PRESS	6.42	Adeq Precision	15.821

Table3.3: GOF statistics for electrode melting rate

The goodness of fit measures the strength and adequacy of the quadratic model. The results obtained shows that the model has 95% capacity to predict the electrode melting rate when any change occurs in any of the input parameters

To check for errors in the data collected for analysis a statistical computation is done to check for outliers and the cooks distance is employed to check for this The generated cook's distance for electrode melting rate is presented in Figures 3.1

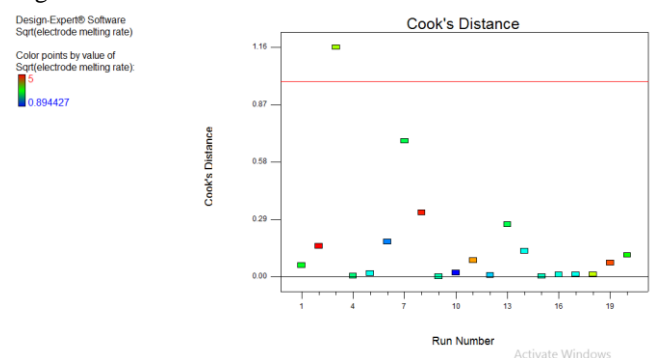


Figure 3.2: Generated cook's distance for electrode melting rate

The cook's distance figure 3.2 shows that one outlier exist in the data but the rest of the data are statistically significant as they all fall within the range 0 and 1 the outlier can be deleted from the data and ignored.

To determine the most appropriate power transformation to apply to a response data The Box Cox plot is required. Most data transformations can be described by the power function,  $y = \mu + \sigma \epsilon$ , where  $\sigma$  is the standard deviation,  $\mu$  is the mean and  $\alpha$  is the power. Lambda is 1 -  $\alpha$  in all cases. If the standard deviation associated with an observation is proportional to the mean raised to the  $\alpha$  power, then transforming the observation by the  $1 - \alpha$  (or  $\alpha$ ) power gives a scale satisfying the equal variance requirement of the statistical model. The box cox plot for the electrode melting rate is shown in figure 3.3

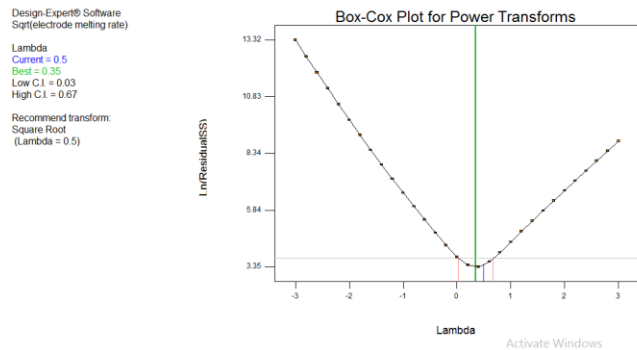


Figure 3.3: box cox plot for electrode melting rate

The optimal equation which shows the individual effects and combine interactions of the selected input variables (current, voltage and gas flow rate) against the mesured electrode melting rate is presented based on the actual values in figure 3.4

**Final Equation in Terms of Actual Factors:**

$$\begin{aligned} \text{Sqrt}(\text{electrode melting rate}) = & \\ & +126.24256 \\ & -1.38048 * \text{current} \\ & +2.82716 * \text{voltage} \\ & -6.63498 * \text{gas flow rate} \\ & +0.011636 * \text{current} * \text{voltage} \\ & +4.18099\text{E-}004 * \text{current} * \text{gas flow rate} \\ & +0.17299 * \text{voltage} * \text{gas flow rate} \\ & +3.54726\text{E-}003 * \text{current}^2 \\ & -0.19126 * \text{voltage}^2 \\ & +0.17733 * \text{gas flow rate}^2 \end{aligned}$$

Figure 3.4: optimal equation for minimization of electrode melting rate

The response surface shows a 3D plot of the combined interaction between two input variables and the output To study the effects of current and gas flow rate on the electrode melting rate, 3D surface plots presented in Figure 3.4 was generated as follows:

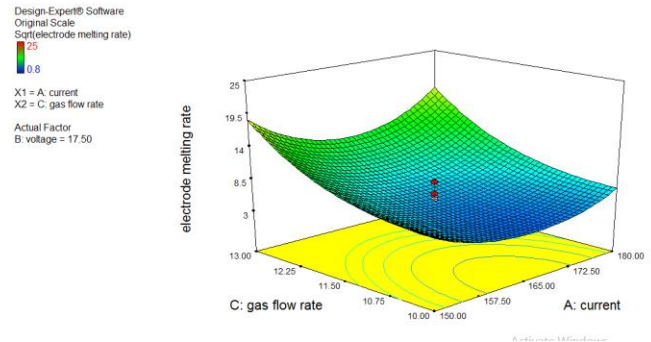


Figure 3.5: Effect of gas flow rate and current on electrode melting rate

The surface plots in figure 3.5 shows that the combined interaction between current and gas flow rate has a significant effect on the minimization of the electrode melting rate., a reduction in gas flow rate will lead to corresponding decrease in the electrode melting rate. The final optimal solution was obtained showing optimal results for current, voltage, gas flow rate that will produce the minimum electrode melting rate as shown in table 3.4.

	Current	voltage	gas flow rate	fume conc	electrode melting rate	Desirability
1	168.25	16.00	10.00	2.57348	3.07436	0.911
2	167.21	16.00	10.00	2.73064	3.07498	0.907
3	166.99	16.00	10.00	2.76517	3.07857	0.906
4	166.70	16.00	10.00	2.81161	3.08516	0.900
5	168.01	16.00	10.02	2.53183	3.05294	0.896
6	166.02	16.00	10.00	2.92333	3.10869	0.893
7	168.64	16.01	10.00	2.52226	3.09011	0.892
8	168.56	16.00	10.05	2.34982	3.03381	0.890
9	172.38	16.00	10.00	2.05195	3.34377	0.888
10	169.41	16.00	10.10	2.11013	3.02754	0.885

Table 34: Optimal solutions of numerical optimization model

#### IV. CONCLUSION

Various process parameters affecting electrode melting rate and safe welding fumes its experimental data suitability and statistical integrity has been examined and presented in this paper. The results obtained showed that the reduction of gas flow rate will help to control the electrode melting rate as well as the fume formation rate. The response surface methodology has been applied to examine the influence of TIG welding process parameters on the safe welding fumes. The box cox plot was used to detect for any power transformation, the square root power transform was the best fit for the model developed, the model developed possessed a very high goodness of fit of about 95% determination strength. The model developed has explained that critical control of gas flow rate is of great importance to reduce the electrode melting rate as well as the fume concentration in TIG welding.

#### REFERENCES

[1] Villaume, J.E., Wasti, K., Liss-Suter, D., and S. Hsiao (1979) Effects of Welding on Health, Miami, FL. American Welding Society.

- [2] Kim, J.Y., Chen, J.C., Boyce, P.D., and D.C. Christiani (2005) Exposure to Welding Fumes is Associated with Acute Systemic Inflammatory Responses. *Occup Environ Med.* 62(3):157-163.
- [3] Wallace, M., Shulman, S., and J. Sheehy (2001) Comparing Exposure Levels by Type of Welding Operation and Evaluating the Effectiveness of Fume Extraction Guns. *Appl. Occup. Env. Hyg.* 16(8): 771-779.
- [4] United States Environmental Protection Agency (1994) Development of Particulate and Hazardous Emission Factors for Electric Arc Welding (AP-42, Section 12.9). Research Triangle Park, NC.
- [5] Voitkevich, V. (1995) Welding Fume Properties. In *Welding Fumes - Formation, Properties, and Biological Effects*. Cambridge, England: Abington 18-71.
- [6] Antonini, J.M., Taylor, M.D., Zimmer, A.T., and J.R. Roberts (2004) Pulmonary Responses to Welding Fumes: Role of Metals Constituents. *J Toxicol Environ Health* 67(3):233-249.
- [7] Liden, G., and J. Surakka (2009) A Headset-Mounted Mini Sampler for Measuring Exposure to Welding Aerosol in the Breathing Zone. *Ann. Occup. Hyg.* 53(2):99-116.
- [8] Antonini, J.; Lewis, A.; Roberts, J.; Whaley, D. Pulmonary effects of welding fumes: Review of worker and experimental animal studies. *Am. J. Ind. Med.* 2003, 43, 350–360.
- [9] Lu, W.; Howarth, A.; Adam, N.; Riffat, S. Modelling and measurement of airflow and aerosol particle distribution in a ventilated two-zone chamber. *Build. Environ.* 1996, 31, 417–423.
- [10] Ashburner, L. 1989. Some hazards of welding fume. *Joining and Materials* 2(3): 118, 119.
- [11] NIOSH. 1988. Criteria for a recommended standard – welding, brazing, and thermal cutting. NIOSH document no. 88-110. Cincinnati, Ohio.
- [12] Pekkari, B. 2000. Growing concerns about health, safety and environment in welding. *Welding in the World* 44(6).
- [13] Voitkevich, V. 1995. *Welding Fumes: Formation, Properties and Biological Effects*. Cambridge, England: Abington Publishing.